Electromagnetic forces of the cage rotor in conical whirling motion

A. Tenhunen[1], T. Benedetti[1], T. P. Holopainen[2] and A. Arkkio[1]

[1] Laboratory of Electromechanics
Helsinki University of Technology
P.O. Box 3000, FIN-02015 HUT, Finland
phone: +358 9 451 2382
fax: +358 9 451 2991
e-mail: Asmo.Tenhunen@hut.fi

[2] VTT Industrial Systems
Technical Research Centre of Finland
P.O. Box 1705, FIN-02044 VTT, Finland
e-mail: Timo.Holopainen@vtt.fi

Abstract

The paper deals with the electromagnetic forces in induction machines when the rotor is in cylindrical whirling motion, symmetric conical whirling motion or combination of them. These motions describe the eccentric movements of the rigid rotor in induction machines. The time stepping finite element analysis is used for solving the magnetic field, and the forces are calculated from the air gap by a method based on the principle of virtual work. The forces are measured for a test motor equipped with active magnetic bearings. The active magnetic bearings are used to generate the eccentric rotor motions and also to measure the electromagnetic forces. The computed and calculated forces show relatively good agreement. Based on the calculated and measured results, a simple analytical model is developed to describe the electromagnetic forces of the rigid rotor motions.

1. Introduction

The electromagnetic force acts between the rotor and stator when the rotor is not perfectly concentric and aligned with the stator. In this paper, the forces are studied during different kind of eccentric motions of the rigid rotor. The eccentric motions of the rigid rotor are divided into two basic modes, cylindrical whirling motion and symmetric conical whirling motion. The cylindrical whirling motion of the rotor means that the rotor remains aligned with the stator but the geometrical centreline of the rotor travels around the geometrical centreline of the stator in a circular orbit with a certain frequency known as a whirling frequency, and with a certain radius, known as the whirling radius. The symmetric conical whirling motion of the rotor means that the whirling radius at each end of the rotor is equal but in opposite directions and the whirling frequency remains constant. These modes of rotor motions and a combination of them are illustrated in Fig. 1.

To simplify the task, the present work focuses on the first harmonic force component i.e. the force at the whirling frequency. Also, for simplicity, only the rigid rotor motions are considered i.e. the bending of the rotor is neglected.

Conventionally the electromagnetic forces acting between the rotor and stator have been studied

analytically [1-4]. Most of these studies focused on two special cases of the whirling motion, i.e. static and dynamic eccentricity. Früchtenicht et al. [5] derived equations for the forces in induction machines in general whirling motion. Arkkio et al. [6] studied the forces in whirling motion by finite element analysis and verified their results by measurements. They also presented a low order force model, which presents the forces as a function of whirling frequency, assuming that the force is linear function of the displacement. Tenhunen et al. [7] utilised the spatial linearity property of the forces by calculating the forces as a function of the whirling frequency from the impulse response of the rotor displacement.
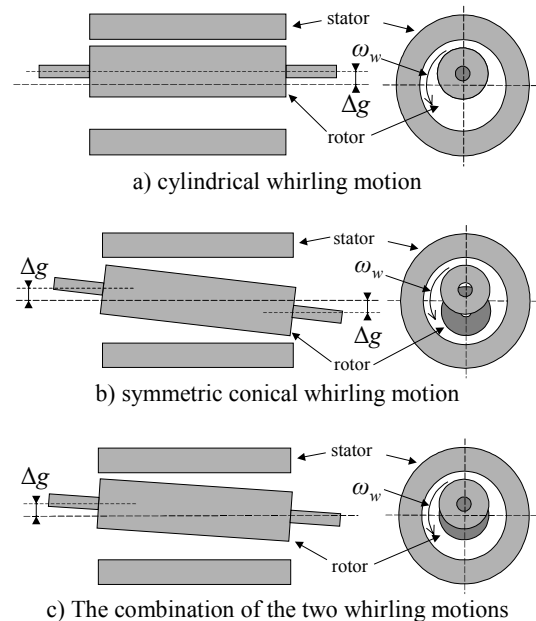

a) cylindrical whirling motion

b) symmetric conical whirling motion

c) The combination of the two whirling motions

Figure 1. Studied types of rigid rotor motions as in Ref. [9]. In figures Δg is the whirling radius of the rotor.

The references given above focus on the type of eccentricity in which the rotor is aligned with the stator. Dorrell [8,9] developed analytical tools to study the forces for the static and dynamic eccentricity of the conical motion. His model includes the effects of equalising currents, which he studied in [10]. He concludes that in the conical motion of the rotor, no equalising currents occur in the stator windings or in the rotor cage. Tenhunen [11] studied the effects of the equalising currents on the forces for the same types of eccentricity by finite element analysis.

The aim of the study is to investigate the superposition for the forces when the rotor is performing combined cylindrical and conical whirling motion. This means that the forces calculated for the cylindrical and conical motion can be combined and the result is the forces for the combined motion.

2. Methods of analysis

2.1 Methods of numerical analysis

The 2D time stepping, finite element analysis has been shown to be good and accurate tool to study the electromagnetic force on a cylindrical whirling cage rotor [6]. When the rotor is not parallel with respect to the stator, the variations of the magnetic field in the axial direction have to be included in a way or another into the analysis. The use of 3D FEM is one solution, but the size of the problem and computation times limits the use of 3D modelling. Alternative way is use multi-slice finite element analysis, which is used to model the effects of rotor skewing in induction motors [12]. In the multi-slice model, the 3D effects are included into the 2D FEM by taking a set of cross sections of the motor perpendicular to the stator shaft and solving the magnetic field in each slice.

In this study, the calculation of the operating characteristics of the induction motor is based on time-stepping, multi-slice, finite element analysis of the magnetic field. The details of the method have been presented in Reference [13].

In the multi-slice modelling, the motor is divided into the slices cut by planes perpendicular to the stator axis. The slices are connected together by forcing the currents in the stator windings and rotor cage to be continuous from slice to slice. The magnetic field in the core region of the slice of the motor is assumed to be two-dimensional, and the two-dimensional field equation is discretised by the finite element method. The effects of end region fields are taken into account approximately by constant end-winding impedances in the circuit equations of the windings. The field equation and the circuit equations are solved together as a system of equations. The time-dependence of the field is modelled by Crank-Nicholson method. The magnetic field, the currents and the potential differences of the windings are obtained in the solution of the coupled field and circuit equations.

The method based on the principle of virtual work presented by Coulomb [14] is used to compute the electromagnetic forces. In the two-dimensional formulation, the force is obtained as a surface integral over the finite elements in the air gap.

The motion of the rotor is obtained by changing the finite element mesh in the air gap. The cylindrical whirling motion of the rotor is modelled using one slice, which is equivalent with conventional finite element analysis. The analysis of the symmetric conical motion is done using three slices with equal length in the multi-slice model. The relative eccentricity ε_n at the centre point of the rotor at each slice is defined as

$$\varepsilon_n = \frac{2n - n_{tot} - 1}{n_{tot}} \varepsilon \qquad (1)$$

in which n is index of the slice, n_{tot} is total number of slices and ε is the relative eccentricity in the ends of the motor. The relative eccentricity ε is defined as a ratio between the whirling radius and the length of the air gap. The total number of slices was chosen to be three, which is minimum value to get acceptable results [12]. Bigger number of slices would improve the accuracy but the size of the problem may become too large to solve. We used second-order, isoparametric, triangular elements and a typical finite element mesh for one cross section of the motor contained about 10000 nodes.

The impulse method in the finite element analysis is utilised in the calculation of the forces between the stator and the rotor. The details of the impulse method are presented in reference [7]. The basic idea of the impulse method is to move the rotor from its central position for a short period of time to one direction, fixed into the stator co-ordinate system. This displacement excitation disturbs the flux density distribution in the air gap, and by doing this, produces forces between the rotor and stator. Using spectral analysis techniques the frequency response function of the force is determined using the excitation and response signals.

The length of the rectangular displacement pulse in the simulation was 0.01 s. The amplitude of the static pulse was 11% of the air gap length for the whirling and the conical modes and 22% for the combined motion. Total simulation time was 1.0 s with constant time-step of 0.05 ms. To increase the spectral resolution, the sample size was extended to be 2 s obtained by adding zeros to the end of the sample leading to frequency resolution of 0.5 Hz. The discrete excitation and force signals were transformed into the frequency domain by the fast Fourier transform without filtering or windowing. The number of sample points was 8192.

The frequency response function presents the electromagnetic forces per whirling radius as a function of whirling frequency. Then, with the spatial linearity property of the forces, the frequency response defines the forces for a specific whirling radius for the studied whirling frequency range. The spatial linearity property of the forces is used in this study. Analytically, the spatial linearity is shown to be valid for small values of eccentricity [5] and also numerically [14] it is shown to be valid at least until 40 % eccentricities.

2.2 Methods of measurements

Parameter	
Number of poles	4
Number of phases	3
Number of parallel paths	1
Outer diameter of stator [mm]	235
Core length [mm]	195
Inner diameter of stator [mm]	145
Airgap length [mm]	0.45
Number of stator slots	36
Number of rotor slots	34
Connection	Delta
Skew	0
Rated voltage [V]	380
Rated frequency [Hz]	50
Rated current [A]	28
Rated power [kW]	15
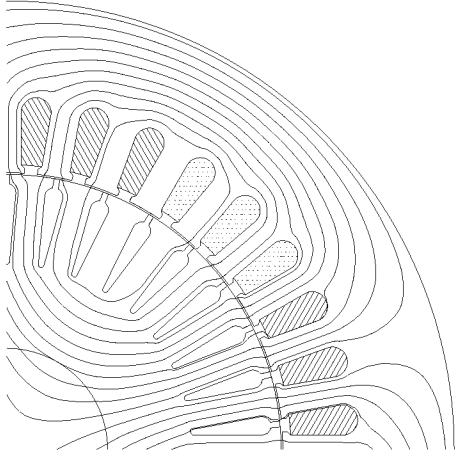
Figure 2. The cross-sectional geometry of the test motor.

The test machine is a 15 kW four-pole cage induction motor. The main parameters of the motor are given in Table I and the cross-sectional geometry is shown in Fig. 2. The test motor was equipped with radial magnetic bearings to measure the forces and to generate the eccentric motions of the rotor. Only the radial bearings were installed, because the electrical machine itself acts as an axial bearing. The radial bearings were ordinary eight-pole heteropolar bearings with bias-current linearisation. Magnetic-bearing operation and the parameters of this particular bearing type are listed by Lantto [15].

The calibration of the active magnetic bearings and the measurements were done following the procedure presented in [6]. The axial rotor geometry of the test motor is shown in Fig. 3. To get the pure conical motion in the measurement, one extra calibration was done. The trajectory of the rotor was determined in such a way that the total force acting on the rotor was zero (i.e. $F_1 = -F_2$). Then, the centre point of the rotor is concentric and the conical motion causes only the moment acting on the centre point of the rotor.
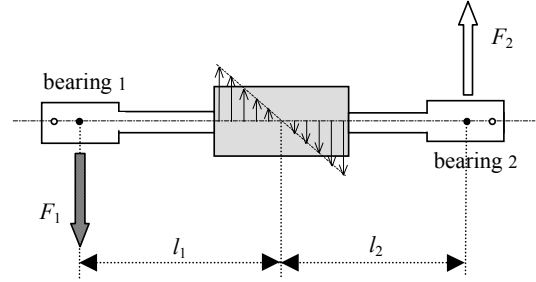

Figure 3. Axial rotor geometry of the test machine
● centres of bearing magnets
○ centres of position sensors
→ magnetic forces acting on the rotor
⇒ reaction of the magnetic bearings

The measured total force F acting on the rotor during the eccentric motion and the moment M acting at its centre are measured through the forces F_1 and F_2 acting on the magnetic bearings, using the basic lows of mechanical equilibrium

$$F = F_1 + F_2$$
$$M = F_1 l_1 + F_2 l_2$$
(2)

where F_1 and F_2 are the measured forces applied in the centre points of the bearing magnets and $l_1 = 0.2725$ m and $l_2 = 0.2475$ m are the distances of these two points from the centre point of the rotor.

The motor is running at no load and supplied by sinusoidal 230 V three-phase voltage. It was necessary to reduce the voltage level from the rated 380 V to keep the magnetic bearings at the linear range of operation to guarantee accurate force measurements. Because of the small clearance available between the ends of the shaft and the touch-down bearings near to the magnetic bearings, a whirling radius $\Delta g = 20\mu$m (i.e. about 4.4 % of the air gap) was chosen.

3 Calculated and measured results

3.1 Cylindrical whirling motion

The whirling cage rotor creates the electromagnetic force between the rotor and the stator. According to analytical theory [5], the force vector has the same frequency as the whirling motion. If the force vector is divided into a radial component in the direction of the shortest air gap and a tangential component perpendicular to the radial one, the components are almost independent on time [6]. Fig. 4 shows the radial and tangential components of the force computed and measured as a function of whirling frequency. The motor is running at no load and supplied by 230 V voltage. The whirling radius is 20μm. The agreement between the measured and calculated results is good.
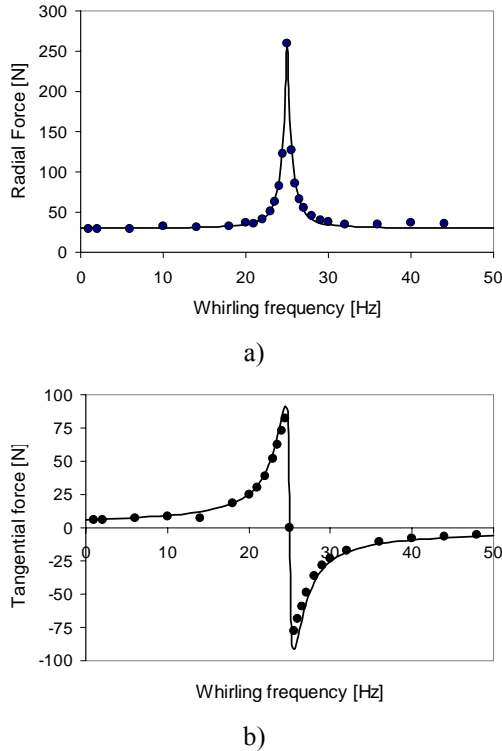
a)

b)

Figure 4. The radial and tangential components of the force as a function of the whirling frequency.
a) Radial
b) Tangential
Continuous line is calculated and the measured ones are marked by ●.

The rotor eccentricity produces two harmonic components into the flux distribution. Usually these harmonics rotate at speed different from the speed of the rotor and thus, they induce eddy currents in the rotor cage. The currents oppose the change of the flux and thus equalise the flux distribution and reduce radial force. At 25 Hz whirling frequency, both of the eccentricity harmonics has zero slip with respect to the rotor. In this case no equalising currents occur in the rotor cage and maximum force occurs.

3.2 Symmetric conical whirling motion

The forces for the symmetric conical whirling motion of the rotor are calculated for each of the three slices in the multi-slice FEA. Fig. 5 shows the radial components of the force acting on the centre point of each slice. The tangential components of the forces are almost zero (less than 0.02 N) in the studied frequency range. The motor was running at no-load and supplied by sinusoidal 230 V three-phase voltage. The whirling radius at both ends of the motor was 20μm.

Now, the equalising currents, which try to be induced in one end of the rotor cage have same amplitude but opposite direction compared with the currents try to be induced in the other end of the motor. As a result, no equalising currents occur in rotor cage and the force is almost constant in the studied whirling frequency range.
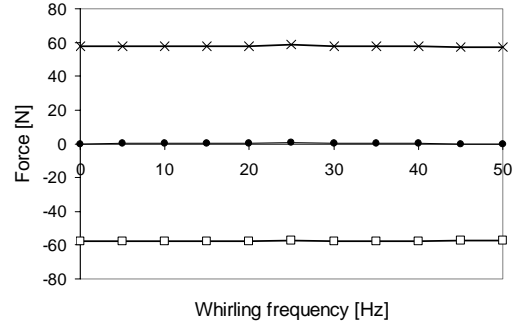

Figure 5. Calculated forces of the slices for conical motion of the rotor with whirling radius 20 μm.
—×— is the force of the first slice
—●— is the force of the second slice (concentric one)
—□— is the force of the third slice.

Fig. 6 shows the calculated radial forces of one slice as functions of relative eccentricity during the conical motion of the rotor. The whirling frequency is $\omega_w = 0$ Hz, i.e. static conical eccentricity, and slip and supply voltage have been used as a parameter. The radial forces increase linearly with the whirling radius.
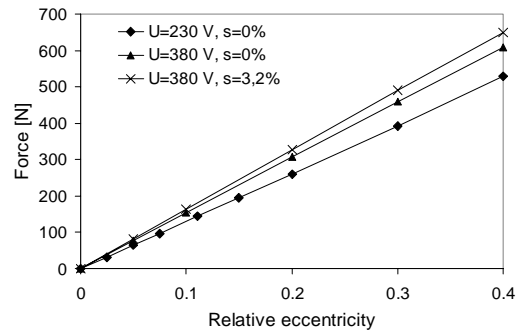

Figure 6. The amplitude of the radial force of one slice as a function of relative eccentricity ε during the conical motion at ω_w=0 Hz, at different voltages and slips.

Since, in the measurement of the forces for the symmetric conical whirling motion of the rotor, described in section 2.2, the result is the moment M acting on the centre point of the rotor, the results of the calculations are also presented by moment M, to enable the comparison of the results.
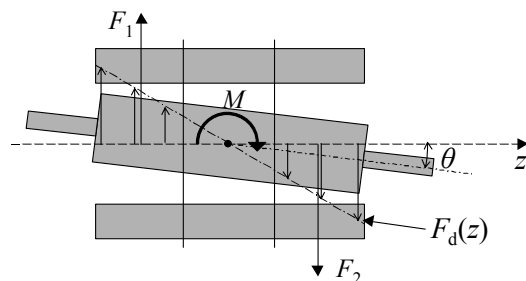

Figure 7. The forces F_1 and F_2 of the slices, force distribution $F_d(z)$ and moment M in conical mode motion.

Supposing that the forces have a spatial linearity property, the forces can be presented by a force distribution $F_d(z) = g'z+k'$ in which the z is the axial position in the shaft and k' and g' are coefficients (Fig.

7). The coefficient g' is related to the force distribution due to the symmetrical conical motion and the coefficient k' is related to the force distribution caused by the cylindrical motion. The force distribution can be defined from the calculated forces acting on the slices

$$F_n = \int_a^b F_d(z)dz = \int_a^b g'z + k'dz \qquad (3)$$

where F_n is the force acting on the slice n and b and a are the ends of the slice. The coefficients k' and g' are solved using Equation (3) and calculated forces of the slices. The moment M at the centre point of the rotor is then defined as

$$M = \int_{-\frac{l}{2}}^{\frac{l}{2}} F_d(z)zdz \qquad (4)$$

in which l is the length of the rotor. Figure 8 shows the calculated and measured moments acting on the rotor. The rotor is performing the symmetric conical whirling motion with whirling radius of 20 μm. The motor was running at no load and supplied by 230 V voltage.
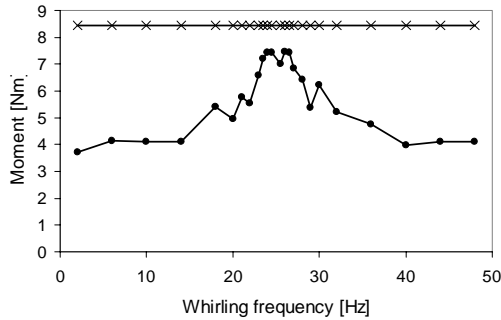

Figure 8. Moments in symmetric conical whirling motion with whirling radius 20 μm.
—●— measured
—x— calculated

The calculated moment is almost constant in the studied frequency range. Near to the whirling frequency 25 Hz, the measured moment is quite near to the calculated one. At the other frequencies the measured moment is notably smaller and seems to have a bit the same frequency dependence as the radial force in cylindrical motion. The explanation for this behaviour may be the interbar currents. The test motor has an aluminium cast cage rotor. The resistance between the bars through the rotor sheet stack is not infinite, and equalising currents can flow in the end parts of the rotor cage through the rotor stack from bar to bar. This may explain the damping effects seen in Fig. 8.

3.3 Forces in combined motion

So far we have studied the basic modes of the rigid rotor motions. The next step is to calculate the forces caused by the combined cylindrical and conical motions of the rigid rotor. Fig. 1 c) presents the combined eccentric motion in which one end of the rotor is concentric and the other one is performing whirling motion with 40 μm whirling radius. This motion presents combination of the cylindrical whirling motion with radius 20 μm and the symmetric conical whirling motion with whirling radius 20 μm, for which the forces and moments are shown in sections 3.1 and 3.2. The motor is running again at no load and supplied by 230 V voltage. Fig. 9 shows the calculated forces for each slice as a function of whirling frequency.
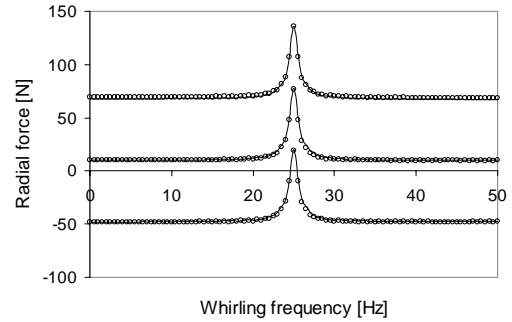
a)
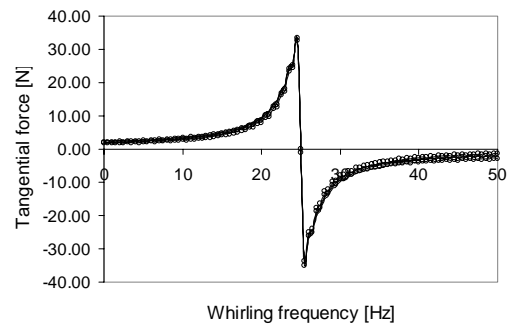
b)

Figure 9. a) the radial and b) the tangential component of the forces of each slice as a function of whirling frequency. Continuous line is calculated forces and the sum of separately calculated forces for the cylindrical and the conical motions are marked by ○.

Because this motion is a combination of the cylindrical and conical motions, we added the separately calculated forces for each slice. The results are shown in Fig. 9 by ○.

If the total force is calculated by adding the slice forces, the result is equal with the calculated force in cylindrical motion (shown in Fig. 4). And if the moment applied in the centre point of the rotor is calculated using Equations (3) and (4) the result is equal to the calculated moment for conical motion.

The measured forces in the magnetic bearings have to be presented striclty in terms of total force and moment. The total force between the rotor and stator is almost the same as in cylindrical motion (Fig. 10). The measured moment is a bit higher for the combined motion than for a symmetric conical motion. The reason is that the measured bearing forces of cylindrical motion have a small component of moment corresponding 2 μm conical

motion. If the moments of cylindrical and conical motions are summed up, the result has good agreement with the moment of the combined motion. Fig. 11 shows the measured moment as a function of whirling frequency for the combined motion (marked by x) and for the sum of the moments of the whirling and the conical motion (marked by ●).
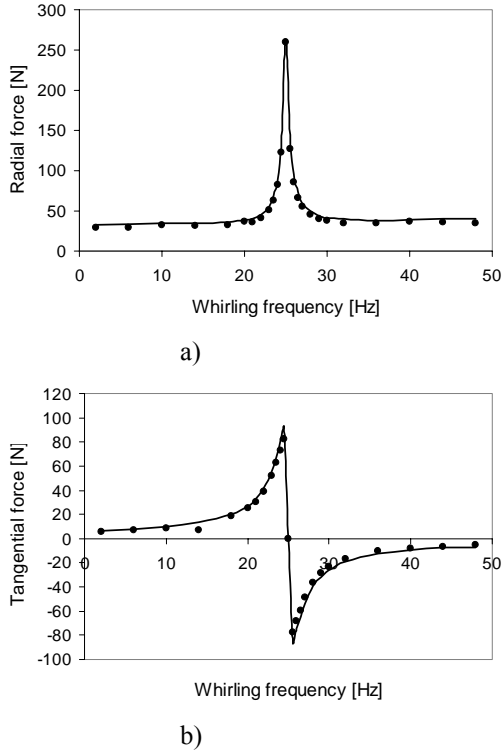

a)

b)

Figure 10. a) the radial and b) the tangential component of the force as a function of whirling frequency. Continuous line is measured forces for combiend motion and the sum of separately measured forces for the cylindrical and the conical motions are marked by ●.
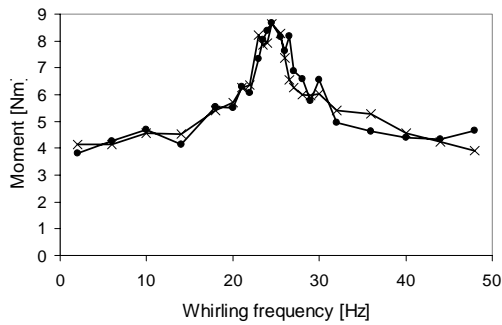

Figure 11. The measured moment as a function of whirling frequency for combined motion (marked by x) and for the sum of the moments of the cylindrical and the conical motion (marked by ●).

3.4 Low-order force model

The force distribution $F_d(z)$ describes well the electromagnetic forces caused by eccentric motions of the rigid rotor. The results presented above indicate that the shorter expression is received by presenting the forces in terms of total force acting between the rotor

and stator and the moment acting on the centre point of the rotor

$$
\begin{bmatrix} F(j\omega_w) \\ M(j\omega_w) \end{bmatrix} = \begin{bmatrix} K(j\omega_w) & \\ & G \end{bmatrix} \begin{bmatrix} p_c(j\omega_w) \\ \theta(j\omega_w) \end{bmatrix} \tag{5}
$$

where j is imaginary unit, ω_w is the whirling frequency, θ is the angle of the rotor with respect to the stator (i.e. the angle of the conical motion) and p_c is the whirling radius of the centre point of the rotor. The both the angle θ and p_c are complex variables including the information of the direction. The complex frequency response function of the force $K(j\omega)$ is defined as [6]

$$
K(j\omega_w) = k_0 + \frac{k_{p-1}}{j\omega_w - z_{p-1}} + \frac{k_{p+1}}{j\omega_w - z_{p+1}} \tag{6}
$$

where k_0, k_{p-1}, k_{p+1}, z_{p-1} and z_{p+1} are the coefficients. The real valued frequency response function of the moment G is constant at a specified operating point of the motor. In Equation (5) it is supposed that the angle θ is very small, then $\tan(\theta) \approx \theta$. The results of the combined motion show that the forces of the both basic motions of rigid rotor; cylindrical, and symmetric conical motion, can be handeled separately, and the results of them can be combined by Equation (5) to reach the forces of the combined motion.

4. Conclusions

The electromagnetic forces acting between the rotor and stator when the rigid rotor is performing eccentric motions is studied. The magnetic field of the induction motor was solved using multi-slice, time-stepping finite element analysis and the forces were computed from the air gap magnetic field. An induction motor was equipped with active magnetic bearings for verifying the calculated forces. The active magnetic bearings were used to create the eccentric motions of the rotor and also to measure the forces. The measured and calculated results have quite good agreement. The results show that the forces of the cylindrical and the symmetric conical motion can be combined and the result is the forces in the combined cylindrical and symmetric conical motion of the rotor.

References

[1]   Freise, W., and Jordan, H.: 'Einseitige magnetische Zugkräfte in Drehstrommaschinen', *ETZ-A*, 1962, **83**, (9), pp. 299-303.

[2]   Ellison, A. J., and Yang, S. J.: 'Effects of rotor eccentricity on acoustic noise from induction machines', *Proc. IEE*, 1971, **118**, (1), pp. 174-184.

[3]   Belmans, R., Vandenput, A. and Geysen, W.: 'Calculation of the flux density and the unbalanced pull in two pole induction machines., *Archiv für Elektrotechnik*, 1987, **70**, pp. 151-161.

[4] Smith, A. C. and Dorrell, D. G.: 'Calculation and measurement of unbalanced magnetic pull in cage induction motors with eccentric rotors. Part 1: Analytical model', *IEE Proc. Electr. Power Appl.*, 1996, **143**, (3), pp. 193-201.

[5] Früchtenicht, J. Jordan, H. and Seinch, H. O.: 'Exzentnzitätsfelder als Urache von Laufinstabilitäten bei Asynchronmachinen, Parts 1 and 2', *Arch. Electrotech* (Germany), 1982, **65**, pp. 271-292.

[6] Arkkio, A. Antila, M., Pokki, K., Simon, A. and Lantto, E.: 'Electromagnetic force on a whirling cage rotor', *IEE Proc. Electr. Power Appl.*, 2000, **147**, (5), pp. 353-360.

[7] Tenhunen, A., Holopainen, T. P. and Arkkio, A.: 'Impulse method to calculate the frequency response of the electromagnetic forces on whirling cage rotors', Proceedings of CEFC'2002, June 2002, Perugia, Italy, pp. 109.

[8] Dorrell, D. G.: 'Modelling rotor eccentricity in cage induction motors with axial variation of eccentricity', in Proceedings of the Universities Power Engineering Conference, UPEC 1995, September 1995, London, UK, pp. 1-4.

[9] Dorrell, D.: 'Modelling of non-uniform rotor eccentricity and calculation of unbalanced magnetic pull in a 3-phase cage induction motors', Proceedings of ICEM 2000, August 2000, Espoo, Finland, pp. 1820-1824.

[10] Dorrell, D. G.: 'The sources and characteristics of unbalanced magnetic pull in cage induction motors with either static or dynamic rotor eccentricity', in Proceedings of Stockholm Power Tech, Volume: Electric Machines and Drives, June 1995, Stockholm, Sweden, pp. 229-234.

[11] Tenhunen, A.: 'Finite-element calculation of unbalanced magnetic pull and circulating current between parallel windings in induction motor with non-uniform eccentric rotor', in Proceedings of Electromotion'01, June 2001, Bologna, Italy, pp. 19-24.

[12] Tenhunen, A. and Arkkio, A.: 'Modelling of induction machines with skewed rotor slots', *IEE Proc. Electr. Power Appl*, 2001, **148**, (1), pp. 45-50.

[13] Coulomb, J. L.: 'A methodology for the determination of global electromechanical quantities from a finite element analysis and its application to the evaluation of magnetic forces, torques, and stiffness', *IEEE Trans. on Magnetics*, 1983, **19**, (6), pp. 2514-2519.

[14] Tenhunen, A., Arkkio, A. and Holopainen, T. P.: 'Spatial linearity of unbalanced magnetic pull in induction motors during eccentric rotor motions', 15th International Conference on Electrical Machines (ICEM 2002) paper number 115, August 2002. Bruges, Belgium, 6 pages.

[15] Lantto, E.: 'Robust control of magnetic bearings in subcritical machines', *Acta Polytech. Scand. Electr. Eng. Ser.*, 1999, **94**, pp. 143.